

Modulated surface textures for enhanced light trapping in thin-film silicon solar cells

Olindo Isabella,^{1,a)} Janez Krč,² and Miro Zeman¹

¹PVMD/DIMES, Delft University of Technology, P.O. Box 5031, 2600 GA Delft, The Netherlands

²Faculty of Electrical Engineering, University of Ljubljana, Trzaska 25, 1000 Ljubljana, Slovenia

(Received 2 August 2010; accepted 19 August 2010; published online 8 September 2010)

Substrates with a modulated surface texture were prepared by combining different interface morphologies. The spatial frequency surface representation method is used to evaluate the surface modulation. When combining morphologies with appropriate geometrical features, substrates exhibit an increased scattering level in a broad wavelength region. We demonstrate that the improved scattering properties result from a superposition of different light scattering mechanisms caused by the different geometrical features integrated in a modulated surface texture. © 2010 American Institute of Physics. [doi:10.1063/1.3488023]

Light-trapping is an essential approach in thin-film silicon solar cells to increase the effective optical path in thin absorber layers. It uses scattering of light at rough interfaces, introduced into the solar cell by means of substrates coated with a randomly surface-textured transparent-conductive-oxide (TCO) layer.¹ The multijunction approach is widely used in these solar cells.^{2,3} Employing different absorber materials in multi-junction solar cells, such as amorphous silicon alloys and microcrystalline silicon, efficient light trapping is required at long wavelengths (up to 1100 nm). To meet this demand, TCO substrates with different surface textures have recently been developed and tested in solar cells, such as optimized wet-etched⁴ or surface plasma-treated⁵ zinc-oxide, double-textured tin-oxide,⁶ and a combination of etched glass with zinc-oxide.⁷ Even though the potential of using of high performance TCOs has been already investigated,⁸ a physical explanation of why these textures result in high scattering properties is still missing.

In this paper we introduce and analyze a more general concept of surface textures for enhanced scattering in a broad wavelength range, namely a *modulated surface texture*. We demonstrate that the enhanced scattering is achieved by superposition of different scattering mechanisms caused by the different geometrical features integrated in a modulated surface texture.

A substrate with a modulated surface texture can be prepared as a stack of layers in which a different texture is introduced at individual interfaces. Provided the layers are thin enough the textures of the individual interfaces are transferred to a subsequent interface. The resulting surface of the stack accommodates all the morphological components introduced at the individual interfaces. The stack may comprise layers of the same or different materials and a broad range of lateral and vertical geometrical features introduced at interfaces. By combining appropriate geometrical features introduced at the individual interfaces one can take advantage of superimposing the scattering mechanisms caused by these different geometrical features and achieving higher scattering levels in a broad wavelength range in comparison to the scattering contributions from individual morphologies.

When the geometrical dimensions of the rough surface are larger than the wavelength of light, the scattering with strongly directional and weakly wavelength-dependent characteristics can be enhanced. This scattering behavior can be well described by the Mie solution of Maxwell equations.⁹ It is possible to represent such surface-textured morphology as a distribution of spherical particles,¹⁰ so that the diffuse transmittance, T_D , can be described as follows:

$$T_D = \frac{\pi a^2}{L_C^2} Q_{\text{sca}}, \quad (1)$$

where πa^2 is the geometrical cross-section of the distribution-averaged spherical particle of radius a , which is defined as half of the peak-to-peak height of the surface texture; L_C is the correlation length of the surface texture; and Q_{sca} is the scattering efficiency,¹¹ which has a weak wavelength dependency.¹²

When the vertical dimensions of the surface roughness become comparable to the wavelength of light another scattering mechanism becomes dominant. This type of surface exhibits a more diffuse (i.e., less directional) scattering behavior and a significant wavelength dependency. Scalar scattering theory¹³ can be used to approximate this scattering behavior. In this case the T_D can be described as follows:

$$T_D = T_0 \left\{ 1 - \exp \left[- \left(\frac{2\pi\sigma_{\text{rms}}|n_0 - n_1|}{\lambda} \right)^\gamma \right] \right\}, \quad (2)$$

where T_0 is the total (diffuse+specular) transmittance of a rough interface, σ_{rms} is the vertical root-mean-square roughness, n_0 and n_1 are the refractive indices of the materials forming the interface, λ is the wavelength, and γ is the exponent which value ranges from ~ 1.5 to 3 depending on the height distribution function of the surface morphology.^{5,14,15} This scattering mechanism is characterized by a pronounced exponential decay in T_D with increasing wavelength, which is typical for the commonly used randomly surface-textured substrates for thin-film solar cells.

The described principle of surface modulation is given in the inset of Fig. 1, where three sinusoidal-like textures are combined in a modulated texture. In order to quantitatively represent and analyze the morphology of modulated surface textures we use the spatial frequency surface representation,

^{a)}Electronic mail: o.isabella@tudelft.nl.

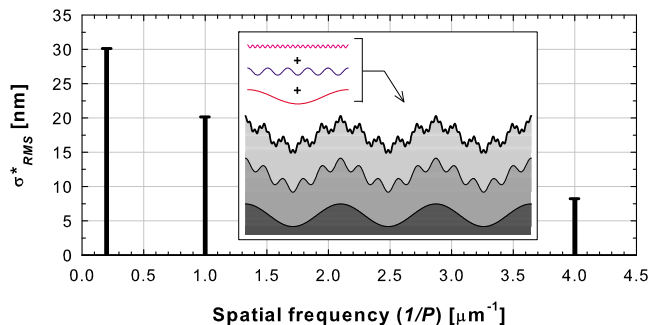


FIG. 1. (Color online) Spatial frequency surface representation of a simple modulated surface.

which is based on the discrete Fourier transform¹⁶ of the surface morphology. From this the spatial frequency distribution of the vertical root-mean-square roughness σ_{rms}^* of the surface can be obtained by multiplying the discrete values of the Fourier amplitude spectrum by $1/\sqrt{2}$. The σ_{rms} value of a surface is a statistical parameter that is widely used to parameterize the roughness of random surface textures, and can be determined from the distribution function, σ_{rms}^* , as follows:

$$\sigma_{rms} = \sqrt{\sum_{i=1}^N [\sigma_{rms,i}^*(f_i)]^2}, \quad (3)$$

where N is the total number of frequency components (f_i) in the spectrum. Both vertical and lateral characteristics of the surface morphology can be efficiently presented using the σ_{rms}^* distribution. In Fig. 1 the spatial frequency representation of the simple example of a modulated surface texture with three sinusoidal-shaped components (one-dimensional sinusoidal-like gratings) is presented. The three vertical bars correspond to the components of spatial frequency at $0.2 \mu\text{m}^{-1}$, $1 \mu\text{m}^{-1}$, and $4 \mu\text{m}^{-1}$, which have σ_{rms}^* discrete values of 30 nm, 20 nm, and 8 nm, respectively. The periods of the sinusoids are related to the spatial frequencies as $P = 1/f$.

We present and analyze the morphological and scattering properties for an example of a designed TCO substrate with a modulated surface texture that can be used in thin-film silicon solar cells. The sample was fabricated by chemically-etching a glass substrate to realize a surface morphology with large feature sizes. Following this, a $1 \mu\text{m}$ thick ZnO:Al TCO layer was deposited using magnetron sputtering¹⁷ and chemically etched to add smaller texture features to the surface roughness. Atomic force microscopy (AFM) was used to determine the morphology and the spatial frequency surface representation of the investigated textures. Due to the isotropic nature of the resulting surface morphologies, a one dimensional discrete Fourier transformation was performed over the profile, which is the combination of line scans over the whole area.

In Fig. 2 AFM scans are shown for the surfaces of etched glass [texture (a)-large features], etched TCO deposited on a flat glass as a reference [texture (b)-small features], and etched TCO on etched glass (the modulated texture). In Fig. 3 the σ_{rms}^* distributions for the three morphologies are shown. In contrast to Fig. 1, Fig. 3 shows that the analyzed textures evolve in a dense distribution of discrete σ_{rms}^* com-

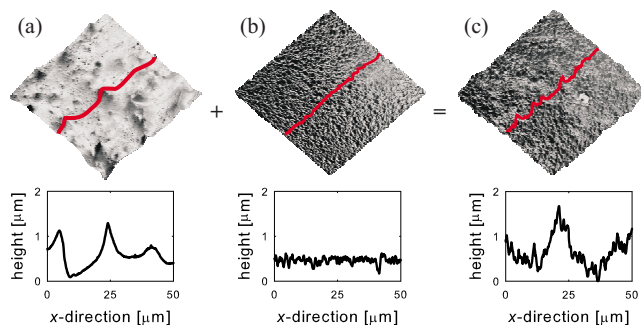


FIG. 2. (Color online) The AFM scans ($50 \times 50 \mu\text{m}^2$ area) and cross sections along x -direction of three different textures: (a) large texture (etched glass, $\sigma_{rms}=200$ nm), (b) small texture (etched TCO on flat glass, $\sigma_{rms}=82$ nm), and (c) the resulting modulated texture (etched TCO on etched glass, $\sigma_{rms}=252$ nm).

ponents. Only the tops of the bars are drawn in the Fig. 3, which results in step-wise σ_{rms}^* curves.

The σ_{rms}^* of the texture (a) (large features) is characterized by a distinct peak at low frequencies, which corresponds to features with large lateral and vertical dimensions (zone 1). This is followed by a decay (zone 2) and then saturation (zone 3). The σ_{rms}^* curve of the texture (b) (small features) does not feature a distinct peak at low frequencies, but instead exhibits a broader distribution of higher values of σ_{rms}^* in zone 2. The sample with a modulated texture shows a high peak in the σ_{rms}^* values at low spatial frequencies due to the contribution of the etched glass, and also higher σ_{rms}^* values over the rest of the spatial frequency spectrum due to the contribution of the etched TCO.

The light scattering properties of the textured substrates were measured using integrating sphere¹⁵ and variable angle spectrometry.¹⁸ The diffuse transmittance of the different surface textures is presented in Fig. 4. Texture (a) exhibits an almost constant T_D over a broad range of wavelengths. We modeled this behavior using Eq. (1) with $a=0.85 \mu\text{m}$, $L_C=5.7 \mu\text{m}$, and Q_{sca} calculated from the distribution of surface features proving that this scattering behavior can be well described by the Mie scattering. The texture (b) exhibits an exponential decay in T_D , which can be modeled using Eq. (2) based on the scalar scattering theory with $\sigma_{rms}=82$ nm, $\gamma=1.5$, and T_0 as determined for the structure. The T_D of texture (b) is decreased at the shorter wavelengths due to absorption in the TCO layer at these wavelengths. The modulated surface texture exhibits the highest T_D across the entire wavelength range. One can observe that the T_D of the modulated surface texture combines the optical behavior of the

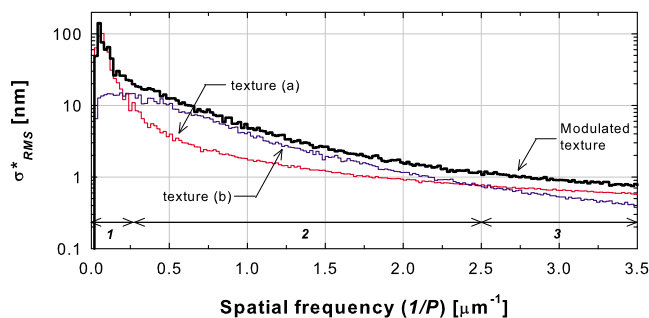


FIG. 3. (Color online) Spatial frequency surface representation (log scale) of texture (a) large features, texture (b) small features and the modulated texture.

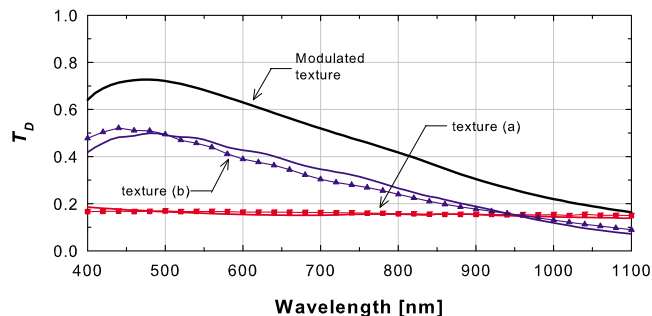


FIG. 4. (Color online) Solid lines: measured T_D of the texture (a) large features, texture (b) small features and the modulated texture. Symbols represent T_D results from the calculations.

individual textures (a) and (b), thus confirming that both scattering mechanisms are present and active.

In Fig. 5 the angular intensity distribution of transmitted light (AID_T), measured in the plane normal to the scattering interface, is shown. The AID_T corresponding to the modulated surface texture has the lowest specular component and the highest diffuse component for almost all scattering angles. The high scattering level results from a combination of the low specular component that originates from the presence of large surface textures, and the broad angular distribution function that comes from scattering at the small surface textures. Therefore two scattering mechanisms, described by Eqs. (1) and (2), are present in the resulting AID_T . The first one contributes to a high scattering level nearby the specular direction and the second one assures an efficient scattering at larger scattering angles. It is this superimposed scattering behavior that is essential for the efficient light trapping in thin-film silicon solar cells. It may be achieved and tailored by surface texture modulation, which can activate several scattering mechanisms.

In this paper we analyzed the scattering properties of a modulated surface texture for application in thin-film silicon solar cells. We demonstrated that the enhanced scattering

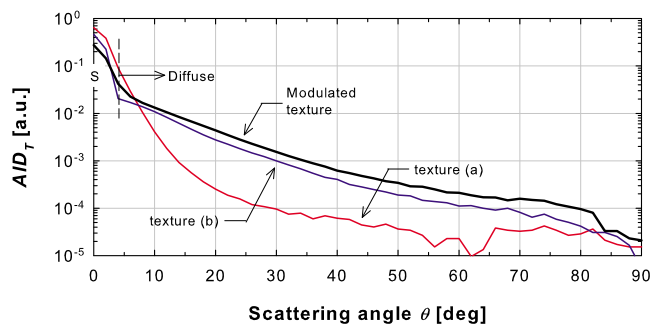


FIG. 5. (Color online) AID_T of texture (a) large features, texture (b) small features, and modulated texture at $\lambda=633$ nm. The letter S indicates the specular component.

levels are achieved by superimposing different scattering mechanisms activated by the different geometrical features integrated in a modulated surface texture. Our example of modulated surface-textured TCO substrate exhibited an increased scattering level across a broad wavelength range up to 1100 nm, and also scattered into large angles. Both of these scattering properties are required for efficient light trapping in multi-junction thin-film silicon solar cells. The scattering behavior of the substrate can be understood by a combination of Mie scattering for larger features, superimposed with the exponential decay of scattered light from smaller features, which can be described by scalar scattering theory. The concept of modulated surface textures represents a promising approach for the design and further understanding of advanced surface textures for solar cell applications.

This work was carried out with a subsidy of the Dutch Ministry of Economic Affairs under EOS-LT program (Project No. EOSLT04029) and Slovenian Research Agency (Grant No. J2-0851-1538-08). The authors thank K. Jäger, R. Santbergen, A. Smets, and T. Temple from the Delft University of Technology for useful discussions.

¹M. Zeman, in *Thin Film Solar Cells: Fabrication, Characterization and Applications*, edited by J. Poortmans and V. Archipov (Wiley, New York, 2006), pp. 173–236.

²T. Söderström, F.-J. Haug, X. Niquille, V. Terrazoni, and C. Ballif, *Appl. Phys. Lett.* **94**, 063501 (2009).

³J. Yang, A. Banerjee, and S. Guha, *Appl. Phys. Lett.* **70**, 2975 (1997).

⁴V. Sittinger, F. Ruske, W. Werner, B. Szyszka, B. Rech, J. Hüpkes, G. Schöpe, and H. Stiebig, *Thin Solid Films* **496**, 16 (2006).

⁵D. Dominé, P. Buehlmann, J. Bailat, A. Billet, A. Feltrin, and C. Ballif, *Phys. Status Solidi (RRL)* **2**, 163 (2008).

⁶M. Kambe, A. Takahashi, N. Taneda, K. Masumo, T. Oyama, and K. Sato, *Proceedings of the 33rd IEEE PVSC*, San Diego (IEEE, New York, 2008), pp. 1–4.

⁷A. Hongsingthong, T. Krajangsang, I. A. Yunaz, S. Miyajima, and M. Konagai, *Appl. Phys. Express* **3**, 051102 (2010).

⁸J. Krč, B. Lipovšek, M. Bokalič, A. Čampa, T. Oyama, M. Kambe, T. Matsui, H. Sai, M. Kondo, and M. Topič, *Thin Solid Films* **518**, 3054 (2010).

⁹G. Mie, *Ann. Phys.* **330**, 377 (1908).

¹⁰J. G. O'Dowd, *Sol. Energy Mater. Sol. Cells* **16**, 383 (1987).

¹¹H. Schade and Z. E. Smith, *Appl. Opt.* **24**, 3221 (1985).

¹²C. F. Bohren and D. R. Huffmann, *Absorption and Scattering of Light by Small Particles* (Wiley, New York, 1983).

¹³P. Beckmann and A. Spizzichino, *The Scattering of Electromagnetic Waves from Rough Surfaces* (Artech House, Norwood, 1987).

¹⁴C. K. Carniglia, *Opt. Eng.* **18**, 104 (1979).

¹⁵J. Krč, M. Zeman, O. Kluth, F. Smole, and M. Topič, *Thin Solid Films* **426**, 296 (2003).

¹⁶J. M. Bennett and L. Mattson, *Introduction to Surface Roughness and Scattering* (Optical Society of America, Washington, D.C., 1989).

¹⁷O. Kluth, A. Löffl, S. Wieder, C. Beneking, W. Appenzeller, L. Houben, B. Rech, H. Wagner, S. Hoffmann, R. Waser, J. A. Anna Selvan, and H. Keppnet, *Proceedings of the 26th IEEE PVSC*, Anaheim, CA (IEEE, New York, 1997), pp. 715–718.

¹⁸P. A. van Nijnatten, *Thin Solid Films* **442**, 74 (2003).